Commun. Comput. Phys.
doi: 10.4208/cicp.181015.270416a

Vol. **20**, No. 2, pp. 374-404
August 2016

Do Current Lattice Boltzmann Methods for Diffusion and Advection-Diffusion Equations Respect Maximum Principle and the Non-Negative Constraint?

S. Karimi and K. B. Nakshatrala*

Department of Civil and Environmental Engineering, University of Houston, USA.

Received 18 October 2015; Accepted (in revised version) 27 April 2016

Abstract. The Lattice Boltzmann Method (LBM) has established itself as a popular numerical method in computational fluid dynamics. Several advancements have been recently made in LBM, which include multiple-relaxation-time LBM to simulate anisotropic advection-diffusion processes. Because of the importance of LBM simulations for transport problems in subsurface and reactive flows, one needs to study the accuracy and structure preserving properties of numerical solutions under the LBM. The solutions to advective-diffusive systems are known to satisfy maximum principles, comparison principles, the non-negative constraint, and the decay property. In this paper, using several numerical experiments, it will be shown that current single- and multiple-relaxation-time lattice Boltzmann methods *fail* to preserve these mathematical properties for transient diffusion-type equations. We will also show that these violations may not be removed by simply refining the discretization parameters. More importantly, it will be shown that meeting stability conditions alone does not guarantee the preservation of the aforementioned mathematical principles and physical constraints in the discrete setting. A discussion on the source of these violations and possible approaches to avoid them is included. A condition to guarantee the non-negativity of concentration under LBM in the case of isotropic diffusion is also derived. The impact of this research is twofold. *First*, the study poses several outstanding research problems, which should guide researchers to develop LBM-based formulations for transport problems that respect important mathematical properties and physical constraints in the discrete setting. This paper can also serve as a good source of benchmark problems for such future research endeavors. *Second*, this study cautions the practitioners of the LBM for transport problems with the associated numerical deficiencies of the LBM, and provides guidelines for performing predictive simulations of advective-diffusive processes using the LBM.

AMS subject classifications: 65-XX

Key words: Lattice Boltzmann method (LBM), meso-scale modeling, multiple-relaxation-time, advection-diffusion equations, comparison principle, maximum principle, non-negative constraint, anisotropy, statistical mechanics.

*Corresponding author. *Email address:* knakshatrala@uh.edu (K. B. Nakshatrala)

 ©2016 Global-Science Press

https://doi.org/10.4208/cicp.181015.270416a Published online by Cambridge University Press

1 Introduction and motivation

The lattice Boltzmann method (LBM) has gained remarkable popularity as a versatile numerical method for fluid dynamics simulations [12]. LBM has its roots in the kinetic theory as opposed to the continuum theory. It needs to be emphasized that LBM solves the Boltzmann equation instead of solving the continuum field equations. On the other hand, the finite element method (FEM) and the finite volume method (FVM) solve the continuum field equations directly. The lattice Boltzmann method has many attractive features, for instance: (1) It can easily handle irregular domains (e.g., unstructured pores and fractures in porous media applications), (2) It is easy to implement even for complicated flow models, (3) It is natural to parallelize even in a heterogeneous computing setup [43]. Some recent advances are extension of LBM to simulate multi-phase flows [20], reactive flows [35], non-linear chemical reactions [2], just to name a few.

Advection-diffusion equation plays a vital role in modeling a variety of physical phenomena. For instance, modeling of reactive-transport [7, 41], simulation of drug delivery in blood [36, 39], transport of chemical species in porous media [4, 29]. Consequently, extension of the LBM to advection-diffusion equation has been the focus of major scientific research. In recent years, several key advancements have been made to extend the LBM to simulate transport phenomena. To name a few: [9, 23, 38, 42, 46]. Of these works, Yoshida and Nagaoka [46], and Huang and Wu [23] have proposed multiple-relaxation-time lattice Boltzmann methods to solve advection-diffusion equations with *anisotropic* diffusivity tensors. However, a numerical method can never be considered attractive for predictive simulations, unless it preserves some (if not all) of the mathematical properties of the equations it is aiming to solve.

The governing equations for transient advective-diffusive systems are parabolic partial differential equations, which possess several important mathematical properties. These properties include the maximum principle and the comparison principle [33, 34], which have crucial implications in modeling physical phenomena. For example, a key consequence of the maximum principle in modeling advective-diffusive systems is the non-negative constraint of the attendant chemical species. Violations of these mathematical properties can make a numerical solution inappropriate for scientific and engineering applications.

It has been shown that many popular finite element and finite volume formulations for diffusion-type equations violate the maximum principle and the non-negative constraint [27,30,32]. Several factors such as the physical properties of the medium, topology of the domain, and the spatial and temporal discretization determine the performance of a numerical solution in preserving the *discrete* versions of the aforementioned mathematical properties. A discussion on the influence of these factors in the context of the finite element method can be found in [30]. Note that a numerical method can be shown to "converge" to the exact solution, but it may not always preserve the mentioned properties. Recently, numerical methodologies have been proposed under the finite element method to satisfy the non-negative constraint and the maximum principle by utilizing

https://doi.org/10.4208/cicp.181015.270416a Published online by Cambridge University Press

the underlying variational structure [32].

Unlike finite element method, LBM does not enjoy a variational structure. LBM is designed to solve the Boltzmann's equation using an explicit finite difference scheme. Hence, advances in preserving the maximum principle under the finite element method may not be readily (if at all) applicable to LBM. Furthermore, LBM is usually shown to be convergent to a hydrodynamic equation through the Chapman-Enskog analysis [10]. However, in a numerical simulation, higher order terms of the Chapman-Enskog analysis will not necessarily vanish. This may result in numerical values that are physically/mathematically invalid. For instance, the mathematical properties mentioned above could be violated.

To the best of our knowledge, the performance of LBM-based formulations for unsteady diffusion and advection-diffusion equations with respect to comparison principles, maximum principles, and the non-negative constraint has not received the attention it deserves. But such a study is of paramount importance, as LBM-based formulations are being employed in predictive numerical simulation of reactive-transport problems. We shall, therefore, put some popular LBM-based formulations to test, and particularly show that these formulations could violate all the aforementioned mathematical principles and physical constraints. The formulations of interest in this paper are the non-thermal Single-Relaxation-Time (SRT) LBM for advection with isotropic diffusion, and the Multiple-Relaxation-Time (MRT) methods for anisotropic diffusion proposed in [46] and [23].

The rest of this paper is organized as follows. Section 2 presents the governing equations for a transient advective-diffusive system along with a brief discussion on the associated mathematical properties. Section 3 reviews the non-thermal single- and multiple-relaxation-time lattice Boltzmann methods for transient diffusion-type equations. In Section 4, several representative test problems are presented with a thorough discussion on the numerical results from LBM-based formulations. Section 5 performs a theoretical analysis on the lattice Boltzmann method to obtain a simple criterion on the time-step and lattice cell size to satisfy the non-negative constraint for isotropic diffusivity. Finally, conclusions are drawn in Section 6. On the notational front, a quantity in the continuous setting will be denoted by upright font (e.g., u), and a quantity in the discrete setting will be denoted by italic font (e.g., u).

2 Unsteady diffusion-type equations

Consider a bounded open domain Ω. We shall denote the boundary of the domain by $\Gamma = \overline{\Omega} - \Omega$, where $\overline{\Omega}$ is the set closure of Ω. We assume that the boundary Γ comprises of two parts $\Gamma^{\mathrm{N}}$and Γ^{D} such that $\Gamma^{\mathrm{N}} \cap \Gamma^{\mathrm{D}} = \emptyset$ and $\Gamma = \Gamma^{\mathrm{N}} \cup \Gamma^{\mathrm{D}}$. We denote the part of the boundary on which Dirichlet boundary condition is prescribed by Γ^{D}. Neumann boundary condition is prescribed on Γ^{N}. A spatial point is denoted by $\mathbf{x}$. The unit outward normal to the boundary is denoted by $\widehat{\mathbf{n}}(\mathbf{x})$. The time interval of interest will be denoted by $[0, \mathcal{T}]$, and the time is denoted by t. The divergence and gradient operators with re-

https://doi.org/10.4208/cicp.181015.270416a Published online by Cambridge University Press

spect to $\mathbf{x}$ are, respectively, denoted by $\mathrm{div}[\cdot]$ and $\mathrm{grad}[\cdot]$. For convenience, we introduce:

$$\mathbf{q}(\mathbf{x},t) := \mathbf{v}(\mathbf{x},t)u(\mathbf{x},t) - \mathbf{D}(\mathbf{x})\mathrm{grad}[u(\mathbf{x},t)], \tag{2.1}$$

$$\mathcal{L}[u(\mathbf{x},t)] := \frac{\partial u(\mathbf{x},t)}{\partial t} + \mathrm{div}[\mathbf{q}(\mathbf{x},t)], \tag{2.2}$$

where $u(\mathbf{x},t)$ is the concentration field. The diffusivity tensor is denoted by $\mathbf{D}(\mathbf{x})$, which is assumed to be symmetric, positive definite, and bounded above. The advection velocity is denoted by $\mathbf{v}(\mathbf{x},t)$, which is assumed to be solenoidal. The initial boundary value problem for a transient advection-diffusion system can be written as follows:

$$\mathcal{L}[u(\mathbf{x},t)] = g(\mathbf{x},t), \qquad (\mathbf{x},t) \in \Omega \times (0,\mathcal{T}], \tag{2.3a}$$

$$u(\mathbf{x},t) = u^{\mathrm{p}}(\mathbf{x},t), \qquad (\mathbf{x},t) \in \Gamma^{\mathrm{D}} \times [0,\mathcal{T}], \tag{2.3b}$$

$$\mathbf{q}(\mathbf{x},t)\cdot\widehat{\mathbf{n}}(\mathbf{x}) = q^{\mathrm{p}}(\mathbf{x},t), \quad (\mathbf{x},t) \in \Gamma^{\mathrm{N}} \times [0,\mathcal{T}], \tag{2.3c}$$

$$u(\mathbf{x},t=0) = u_0(\mathbf{x}), \qquad \mathbf{x} \in \Omega, \tag{2.3d}$$

where the source/sink term is denoted by $g(\mathbf{x},t)$, $u^{\mathrm{p}}(\mathbf{x},t)$ is the prescribed concentration, $q^{\mathrm{p}}(\mathbf{x},t)$ is the prescribed flux, and the initial concentration is denoted by $u_0(\mathbf{x})$. Eq. (2.3a) is a linear parabolic partial differential equation. The initial boundary value problem given by Eqs. (2.3a)-(2.3d) satisfies several important mathematical properties and physical constraints, which will be discussed next.

2.1 Mathematical properties and physical constraints

We introduce the following function space:

$$\mathsf{C}_1^2(\Omega\times(0,\mathcal{T}]) := \left\{ u : \Omega\times(0,\mathcal{T}] \to \mathbb{R} \,\middle|\, u, \frac{\partial u}{\partial t}, \frac{\partial u}{\partial x_i}, \frac{\partial^2 u}{\partial x_i \partial x_j} \in \mathsf{C}(\Omega\times(0,\mathcal{T}]) \right\}, \tag{2.4}$$

where $\mathsf{C}(\Omega\times(0,\mathcal{T}])$ is the set of all continuous functions defined on $\Omega\times(0,\mathcal{T}]$. That is, $\mathsf{C}_1^2(\Omega\times(0,\mathcal{T}])$ contains all the functions in $\mathsf{C}(\Omega\times(0,\mathcal{T}])$ that have continuous first- and second-order spatial derivatives in Ω, and continuous first-order time derivative in $(0,\mathcal{T}]$. We shall define $\mathsf{C}(\overline{\Omega}\times[0,\mathcal{T}])$ to denote the set of functions defined on the set closure of $\Omega\times(0,\mathcal{T}]$.

Property 2.1 (The maximum principle). Let $u(\mathbf{x},t) \in \mathsf{C}_1^2(\Omega\times(0,\mathcal{T}]) \cap \mathsf{C}\left(\overline{\Omega}\times[0,\mathcal{T}]\right)$ be a solution of the initial boundary value problem (2.3) with $\partial\Omega = \Gamma^{\mathrm{D}}$. If $g(\mathbf{x},t) \geq 0$ then

$$\min_{(\mathbf{x},t)\in\overline{\Omega}\times[0,\mathcal{T}]} u(\mathbf{x},t) = \min\left[\min_{(\mathbf{x},t)\in\Gamma\times[0,\mathcal{T}]} u(\mathbf{x},t), \min_{\mathbf{x}\in\Omega} u_0(\mathbf{x}) \right].$$

The maximum principle stated above, implies that the minimum of $u(\mathbf{x},t)$ in domain $\Omega\times[0,\mathcal{T}]$ lies either on the boundary of the domain Ω or is equal to the minimum of the initial value $u_0(\mathbf{x})$ in domain Ω. Also note that for a function $u(\mathbf{x},t)$ that satisfies the assumptions given above, $\min_{\mathbf{x}\in\Omega,t\in[0,\mathcal{T}]} u(\mathbf{x},t) = \max_{\mathbf{x}\in\Omega,t\in[0,\mathcal{T}]}\{-u(\mathbf{x},t)\}$, hence, describing the maximum principle in terms of the min operator is sufficient.

https://doi.org/10.4208/cicp.181015.270416a Published online by Cambridge University Press

Property 2.2 (The comparison principle). Let $u_1(\mathbf{x},t)$ and $u_2(\mathbf{x},t)$ belong to $C_1^2(\Omega\times(0,\mathcal{T}])\cap C\left(\overline{\Omega}\times[0,\mathcal{T}]\right)$. If $\mathcal{L}[u_1]\geq\mathcal{L}[u_2]$ on $\Omega\times(0,\mathcal{T}]$, $u_{0,1}(\mathbf{x},t)\geq u_{0,2}(\mathbf{x},t)$ (i.e., the initial value $u_{0,1}(\mathbf{x},t)$ for $\mathcal{L}[u_1]$ is greater than or equal to the initial value $u_{0,2}(\mathbf{x},t)$ for $\mathcal{L}[u_2]$), and $u_1^p(\mathbf{x},t)\geq u_2^p(\mathbf{x},t)$ on $\Gamma\times[0,\mathcal{T}]$ then $u_1(\mathbf{x},t)\geq u_2(\mathbf{x},t)$ on $\overline{\Omega}\times[0,\mathcal{T}]$.

Mathematical proofs to the maximum principle and the comparison principle can be found in [19]. We now show that the non-negative constraint for the concentration can be obtained as a consequence of the maximum principle under certain assumptions on the input data. One could alternatively obtain the non-negative constraint from the comparison principle, which we will not present here.

Property 2.3 (The non-negative constraint). If $g(\mathbf{x},t)\geq 0$ in Ω, $u^p(\mathbf{x},t)\geq 0$ on Γ, and $u_0(\mathbf{x})\geq 0$ in Ω then $u(\mathbf{x},t)\geq 0\,\forall\mathbf{x}\in\overline{\Omega}$ and $\forall t\in[0,\mathcal{T}]$.

Proof. Based on the hypothesis, we have the following two results:

$$\min_{(\mathbf{x},t)\in\Gamma\times[0,\mathcal{T}]} u(\mathbf{x},t)=\min_{(\mathbf{x},t)\in\Gamma\times[0,\mathcal{T}]} u^p(\mathbf{x},t)\geq 0, \tag{2.5}$$

$$\min_{\mathbf{x}\in\Omega} u_0(\mathbf{x})\geq 0. \tag{2.6}$$

These further imply that

$$\min\left[\min_{(\mathbf{x},t)\in\Gamma\times[0,\mathcal{T}]} u(\mathbf{x},t),\min_{x\in\Omega} u_0(\mathbf{x})\right]\geq 0. \tag{2.7}$$

From the maximum principle, we can conclude that

$$\min_{(\mathbf{x},t)\in\overline{\Omega}\times[0,\mathcal{T}]} u(\mathbf{x},t)\geq 0 \tag{2.8}$$

which gives the desired result that $u(\mathbf{x},t)\geq 0$ in $\overline{\Omega}$ and $\forall t$. □

The following integral will be used in the remainder of this paper:

$$\mathcal{J}_2(u;\Omega;t):=\int_\Omega u^2(\mathbf{x},t)\,d\Omega. \tag{2.9}$$

Property 2.4 (The decay property). If $\mathbf{v}(\mathbf{x},t)=\mathbf{0}$, $u^p(\mathbf{x},t)=0$ on the entire Γ, and $g(\mathbf{x},t)=0$ in Ω then

$$\frac{d}{dt}\mathcal{J}_2(u;\Omega;t)\leq 0\quad\forall t. \tag{2.10}$$

Proof. Noting that $g(\mathbf{x},t)=0$ and $\mathbf{v}(\mathbf{x},t)=\mathbf{0}$, Eq. (2.3a) implies the following:

$$\int_\Omega u\frac{\partial u}{\partial t}\,d\Omega-\int_\Omega u\,\mathrm{div}[\mathbf{D}(\mathbf{x})\mathrm{grad}[u]]\,d\Omega=0. \tag{2.11}$$

https://doi.org/10.4208/cicp.181015.270416a Published online by Cambridge University Press

Using Green's identity and noting that $\mathrm{u}(\mathbf{x},\mathrm{t})=\mathrm{u}^{\mathrm{p}}(\mathbf{x},\mathrm{t})=0$ on Γ, we obtain the following:

$$\int_{\Omega}\mathrm{u}\frac{\partial \mathrm{u}}{\partial \mathrm{t}}\,\mathrm{d}\Omega+\int_{\Omega}\mathrm{grad}[\mathrm{u}]\cdot\mathbf{D}(\mathbf{x})\mathrm{grad}[\mathrm{u}]\,\mathrm{d}\Omega=0. \tag{2.12}$$

Noting that $\mathbf{D}(\mathbf{x})$ is a positive definite second-order tensor, we have:

$$\int_{\Omega}\mathrm{u}\frac{\partial \mathrm{u}}{\partial \mathrm{t}}\,\mathrm{d}\Omega\leq 0. \tag{2.13}$$

This further implies that

$$\frac{\mathrm{d}}{\mathrm{dt}}\int_{\Omega}\mathrm{u}^2(\mathbf{x},\mathrm{t})\,\mathrm{d}\Omega\equiv\frac{\mathrm{d}}{\mathrm{dt}}\mathcal{J}_2(\mathrm{u};\Omega;\mathrm{t})\leq 0. \tag{2.14}$$

In order to obtain the above result, we have assumed that Ω is independent of t, which is the case in this paper. □

In the subsequent sections we will illustrate the performance of some popular LBM-based formulations with respect to the aforementioned mathematical properties in the discrete setting. We will also compare the performance of the lattice Boltzmann method with the finite element method in this regard.

3 The lattice Boltzmann method

The lattice Boltzmann method is a way to numerically solve the Boltzmann equation [21]:

$$\partial \mathrm{f}/\partial \mathrm{t}+\mathbf{v}\cdot\mathrm{grad}[\mathrm{f}]=(\mathrm{f}^{\mathrm{eq}\cdot}-\mathrm{f})/\lambda, \tag{3.1}$$

where f is the distribution of particles in the phase space. The macroscopic velocity is $\mathbf{v}$. The distribution of particles at thermodynamic equilibrium is denoted by $\mathrm{f}^{\mathrm{eq}\cdot}$, λ is the relaxation time and the external force term is neglected for simplicity. Obviously, we have adopted the Bhatnagar-Gross-Krook (BGK) [5] model for the collision term on the right-hand-side of Eq. (3.1). Typically, the velocities are discretized in the way of $DnQm$ lattice models, where n is the number of spatial dimensions and m is the number of discrete momenta. The lattice models of interest in this paper are shown in Fig. 1. These discrete velocity/momentum directions will be denoted by $\boldsymbol{e}_i, i=1,\cdots,m$ and the weight associated to them is w_i, with $\sum_{i=1}^{m}w_i=1$. The time derivative is then discretized using an explicit Euler method. The resulting lattice Boltzmann equation is:

$$\left|f_i\right\rangle(\boldsymbol{x}+\boldsymbol{e}_i\Delta t,t+\Delta t)=\left|f_i\right\rangle(\boldsymbol{x},t)+\boldsymbol{S}(\boldsymbol{x},t)\left(\left|f_i^{\mathrm{eq}}\right\rangle(\boldsymbol{x},t)-\left|f_i\right\rangle(\boldsymbol{x},t)\right), \tag{3.2}$$

where f_i is the discrete distribution of particles with velocity $\boldsymbol{e}_i$ and $\boldsymbol{S}(\boldsymbol{x},t)$ is the $m\times m$ matrix of relaxation times. Also, we have used the notation $\left|\cdot\right\rangle$ to denote $m\times 1$ column

https://doi.org/10.4208/cicp.181015.270416a Published online by Cambridge University Press

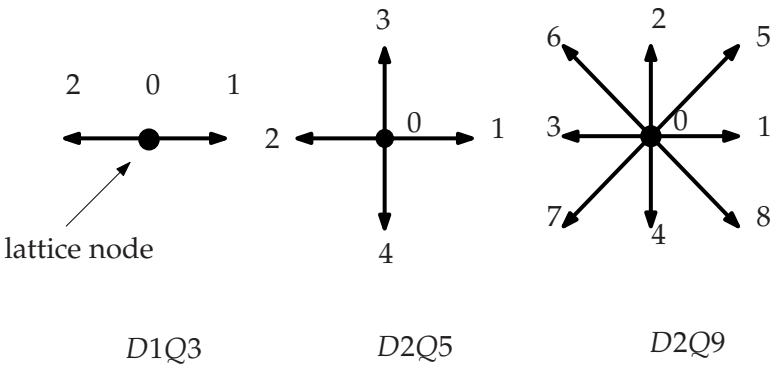


Figure 1: Lattice models employed in this paper.

vector of distributions. The lattice cell size is shown by Δx and time-step is Δt. In the case of Single-Relaxation-Time (SRT) LBM, a popular choice of $\boldsymbol{S}(\boldsymbol{x},t)$ is

$$\boldsymbol{S}(\boldsymbol{x},t)=\frac{1}{\tau}\mathbf{I}_m, \tag{3.3}$$

where $\mathbf{I}_m$ is the $m\times m$ identity matrix and $\tau=\mathrm{D}(\boldsymbol{x},t)/c_s^2\Delta t+1/2$ is the relaxation time. The lattice sound velocity is shown by c_s. A choice of equilibrium distribution for advection-diffusion equation can be

$$f_i^{\text{eq.}}(\boldsymbol{x},t)=w_i u(\boldsymbol{x},t)\left(1+\frac{\boldsymbol{e}_i\cdot\mathbf{v}}{c_s^2}\right), \tag{3.4}$$

where $u(\boldsymbol{x},t)$ is the concentration at a lattice node and w_i is the weight associated with the i-th distribution. This choice of equilibrium distribution is an approximation to the Maxwell-Boltzmann equilibrium distribution [22]. However, SRT LBM does not provide an appropriate framework for advection with anisotropic diffusion equations. For such cases, MRT LBM creates a much more suitable structure. Some recent methods for LBM simulation of anisotropic diffusivity are [23, 46], which we will use in the rest of the paper. For an in-depth treatment and derivation of Eq. (3.2) the reader should consult [18, 22, 43] and references therein. The lattice Boltzmann method can be shown to have a corresponding macroscopic equation as (2.3) using a Chapman-Enskog expansion or asymptotic analysis. The macroscopic quantity of interest in this paper, concentration, can be found as follows:

$$u(\boldsymbol{x},t)=\sum_{i=1}^{m} f_i(\boldsymbol{x},t). \tag{3.5}$$

One of the main issues in numerical simulations using LBM is the implementation of boundary conditions. Since the discrete distributions f_i have more information about the state of matter at each lattice node, translating the macroscopic boundary and initial conditions of Eq. (2.3) to meso-scale is not unique. Hence, there are a multitude of

https://doi.org/10.4208/cicp.181015.270416a Published online by Cambridge University Press

methods for implementing boundary conditions in LBM; e.g. see [11, 40, 49]. Herein, we will consider the following methods for enforcing Dirichlet and Neumann boundary conditions:

(a) *Weighted splitting method for Dirichlet conditions.* In this method, we will replace all the distributions f_i at the lattice node lying near the boundary Γ^{D}. The distributions will be readjusted according to the weights w_i:

$$f_i(\boldsymbol{x},t) = w_i \mathrm{u}^{\mathrm{p}}(\boldsymbol{x},t), \quad \boldsymbol{x} \in \Gamma^{\mathrm{D}}, \tag{3.6}$$

where u^{p} is the prescribed concentration on the boundary.

(b) *Local method for Dirichlet conditions.* In this method, only the unknown distributions will be replaced. Let $\mathcal{U}_{\mathrm{D}}$ be the set of *unknown* distributions and $\mathcal{K}_{\mathrm{D}}$ be the set of known distributions at a point $\boldsymbol{x}$ on boundary Γ^{D}. Then, the unknown distributions will be found as:

$$f_i(\boldsymbol{x},t) = \frac{w_i}{\sum_{j \in \mathcal{U}_{\mathrm{D}}} w_j} \left(\mathrm{u}^{\mathrm{p}}(\boldsymbol{x},t) - \sum_{k \in \mathcal{K}_{\mathrm{D}}} f_k(\boldsymbol{x},t) \right). \tag{3.7}$$

More precisely, the sets $\mathcal{U}_{\mathrm{D}}$ and $\mathcal{K}_{\mathrm{D}}$ can be defined as

$$\mathcal{U}_{\mathrm{D}} = \left\{ i \,\middle|\, \boldsymbol{e}_i \cdot \widehat{\mathbf{n}}(\mathbf{x}) < 0, i = 1, \cdots, m \right\}, \tag{3.8a}$$

$$\mathcal{K}_{\mathrm{D}} = \left\{ i \,\middle|\, \boldsymbol{e}_i \cdot \widehat{\mathbf{n}}(\mathbf{x}) \geq 0, i = 1, \cdots, m \right\}. \tag{3.8b}$$

(c) *Bounce-back method for Neumann conditions.* The unknown distributions will be replaced by the distribution in the opposite velocity direction. Mathematically, this can be written as:

$$f_i(\boldsymbol{x},t) = f_j(\boldsymbol{x},t) - \frac{1}{c_s} \mathrm{q}^{\mathrm{p}}(\boldsymbol{x},t), \quad i \in \mathcal{U}_{\mathrm{N}}, \tag{3.9}$$

where $\boldsymbol{e}_i = -\boldsymbol{e}_j$, $\boldsymbol{x} \in \Gamma^{\mathrm{N}}$ and $\mathcal{U}_{\mathrm{N}}$ is the set of unknown distributions at each point on Γ^{N}.

This concludes our overview of lattice Boltzmann methods for advection-diffusion equations. In the following section we will provide ample evidence that current lattice Boltzmann methods for advection-diffusion equation may lead to violation of mathematical properties of these equations.

4 Representative numerical results

In this section, we employ the single- and multiple-relaxation-time lattice Boltzmann methods to solve representative diffusion and advection-diffusion problems. For brevity, we shall refer to the multiple-relaxation-time method proposed in [46] as the Y-N method,

https://doi.org/10.4208/cicp.181015.270416a Published online by Cambridge University Press

and the method proposed in [23] as the H-W method. In the rest of this section, we shall use the following notation:

$$u_{\min}(t) = \min_{x \in \overline{\Omega}} u(\boldsymbol{x},t), \qquad u_{\max}(t) = \max_{x \in \overline{\Omega}} u(\boldsymbol{x},t). \tag{4.1}$$

In all the problems that utilize MRT LBM, the distributions f_i are initialized according to Eq. (3.4). Note that all the quantities and the equations presented here on are in non-dimensional form.

4.1 One-dimensional problems

4.1.1 Advection and diffusion of Gaussian hill

Consider the domain $\Omega = (-2,2)$, in which the diffusion coefficient is $\mathrm{D} = 10^{-2}$ and advection velocity is $\mathrm{v} = -1$. The source term is taken to be zero over the entire domain. The flux is set to be zero at the boundaries of the domain. The initial concentration is taken to be

$$\mathrm{u}_0(\mathrm{x}) = e^{-(\mathrm{x}-\mathrm{x}_0)^2/\alpha^2}, \tag{4.2}$$

where $\mathrm{x}_0 = 3/4$ and $\alpha^2 = 10^{-3}$ in this problem. We will use a uniform lattice with $D1Q2$ model. SRT LBM will be used to find the numerical solution. The time-step is chosen as $\Delta t = \Delta x^2/6\mathrm{D}$ in all cases to maintain stability. The time interval of interest is $\mathcal{T} = 1/2$. Bounce-back condition is imposed on the boundaries to satisfy the zero flux condition. The initial distributions is assigned to be equal to equilibrium distribution (i.e., $f_i(x,t=0) = f_i^{\mathrm{eq.}}(x,t=0), \forall x \in \Omega$). Since the initial concentration is non-negative throughout the domain, the non-negative constraint implies that the value of concentrations should never be negative in the course of the simulation. Herein, we will show that despite stability and convergence, the numerical solution from LBM may violate the non-negative constraint. We shall use different values of discretization parameters Δx and Δt as given in Table 1. The minimum observed concentration $u_{\min}(t)$ and the error in infinite norm $\mathcal{E}_\infty(t)$ are also shown in Table 1. The error is defined as

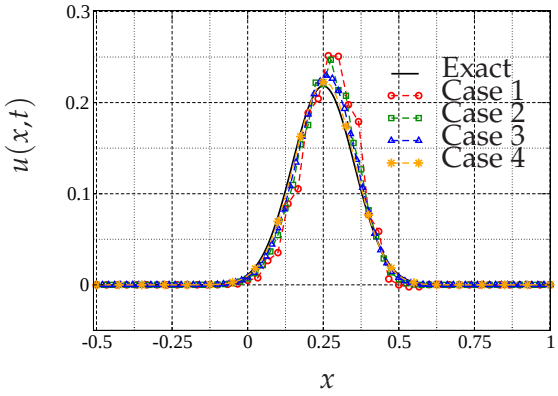
$$\mathcal{E}_\infty(t) = \max_{x \in \Omega} \left| u(x,t) - u_{exact}(x,t) \right|. \tag{4.3}$$

Figs. 2-3 show the numerical results. The violation of the non-negative constraint can be observed. Note that by refining the discretization parameters Δx and Δt, the violations of the non-negative constraint disappear. However, satisfaction of the non-negative constraint is not inherent in the LBM in use for this problem and should not be taken for granted. A computer code for this problem is provided in the Appendix.

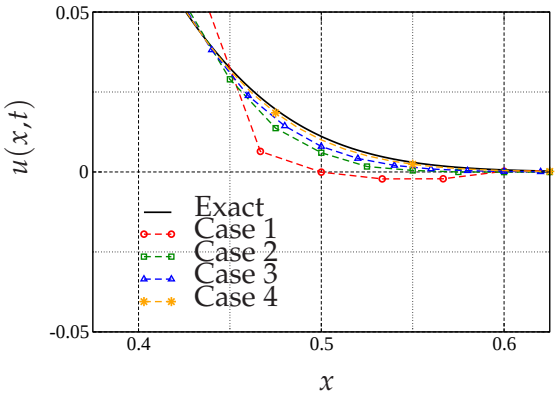
4.1.2 On comparison principle

As stated earlier in this paper, an important mathematical property of advection-diffusion equation is the comparison principle. In the case of linear operator $\mathcal{L}[\cdot]$ in

https://doi.org/10.4208/cicp.181015.270416a Published online by Cambridge University Press



(a) concentration at $t=\mathcal{T}$



(b) a zoomed in view of concentration, showing negative values

Figure 2: Advection and diffusion of Gaussian hill: The concentration at time $t=\mathcal{T}$ is shown. Note the negative values of concentration for Cases 1 and 2. The minimum concentration in Case 1 is -3.9×10^{-3} and in Case 2 it is -3.00×10^{-5}.

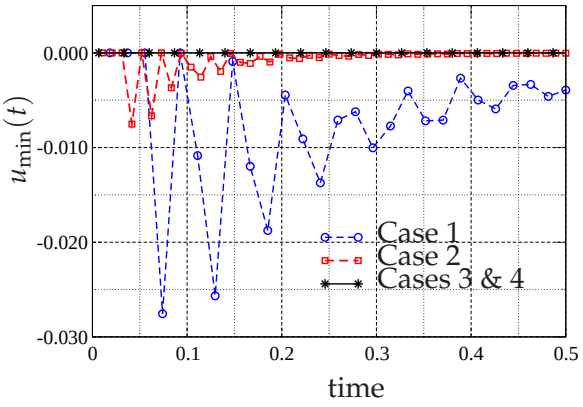


Figure 3: Advection and diffusion of Gaussian hill: Minimum observed concentration is shown against time.

https://doi.org/10.4208/cicp.181015.270416a Published online by Cambridge University Press

Table 1: Advection and diffusion of Gaussian hill: Discretization of time and space domains for the one-dimensional problem. Minimum observed value for concentration, $u_{\min}(t)$ and the error in infinity norm are also provided. Violation of non-negative constraint is obvious.

Case	Δx	Δt	$u_{\min}(\mathcal{T})$	$\mathcal{E}_\infty(\mathcal{T})$
1	3.33×10^{-2}	1.85×10^{-2}	-3.90×10^{-3}	6.50×10^{-2}
2	2.50×10^{-2}	1.04×10^{-2}	-3.00×10^{-5}	4.06×10^{-2}
3	2.00×10^{-2}	6.70×10^{-3}	0.0	2.05×10^{-2}
4	1.25×10^{-2}	2.60×10^{-3}	0.0	7.67×10^{-3}

Eq. (2.2), maximum principle and comparison principle are mathematically equivalent. However, a numerical solution might violate one of the two principles and not the other. Herein, we provide simple numerical examples to demonstrate this issue.

Consider the domain $\Omega=(0,1)$ with prescribed concentration on the boundary:

$$\mathrm{u^p(x,t)}=\begin{cases}\mathrm{u}_L, & \mathrm{x}=0,\\ 0, & \mathrm{x}=1.\end{cases} \tag{4.4}$$

The initial concentration is set to be $\mathrm{u}_0(\mathrm{x})=0, \mathrm{x}\in\Omega$. The diffusion coefficient and the advection velocity are $\mathrm{D}=10^{-3}$ and $\mathrm{v}=1/2$ respectively. We use the $D1Q2$ lattice model and the time-step is $\Delta t=\Delta x^2/6\mathrm{D}$. Fig. 4 shows the numerical result for different values of u_L. The lattice cell size is taken to be $\Delta x=10^{-2}$. Obviously, the maximum principle is violated, since the values of concentration exceeds u_L. However, the comparison principle is not violated (the numerical solution in the entire domain never exceeds the one with larger u_L). Hence, one can conclude that in a discrete setting comparison principle and maximum principle should be accounted for separately.

4.1.3 On choice of lattice model: D1Q2 vs. D1Q3

Consider the domain $\Omega=(0,1)$ in which the diffusion coefficient is $\mathrm{D}=10^{-3}$ and the advection velocity is $\mathrm{v}=1$. We prescribe zero-flux boundary conditions on the entire boundary. The initial condition is

$$\mathrm{u}_0(\mathrm{x})=\begin{cases}1, & \mathrm{x}\in[0.3,0.5],\\ 0, & \text{otherwise.}\end{cases} \tag{4.5}$$

The time interval of interest is $\mathcal{T}=10^{-1}$. Here, we shall compare the performance of two different choices of lattice models with respect to preservation of maximum principle. The lattice models of interest are $D1Q2$ and $D1Q3$ and their discrete velocities and their associated weights are

$$D1Q2:\begin{cases}\boldsymbol{e}=[1,-1],\\ \boldsymbol{w}=[1/2,1/2],\end{cases} \tag{4.6a}$$

$$D1Q3:\begin{cases}\boldsymbol{e}=[0,1,-1],\\ \boldsymbol{w}=[4/6,1/6,1/6].\end{cases} \tag{4.6b}$$

https://doi.org/10.4208/cicp.181015.270416a Published online by Cambridge University Press

The lattice cell size is Δx and the time-step is Δt. The lattice sound velocity for the $D1Q2$ lattice is $c_s = \Delta x/\Delta t$ and for the $D1Q3$ this velocity is $c_s = \Delta x/\sqrt{3}\Delta t$. The distributions will be initialized according to equilibrium distribution.

Using a lattice cell size of $\Delta x = 5\times10^{-3}$ and a time-step of $\Delta t = 4.2\times10^{-3}$, we obtain the numerical results presented in Figs. 5-6. According to the maximum principle, the concentration should remain in $[0,1]$. However, It can be observed that this requirement is violated by both lattice models. Note that in this numerical experiment, concentration exceeds unity and also adopts negative values. Note that the $D1Q2$ and $D1Q3$ give different patterns in $u_{\min}(t)$ and $u_{\max}(t)$. Obviously, the maximum and minimum values of concentration from the $D1Q3$ lattice oscillate more compared to the $D1Q2$ lattice. However, the magnitude of violations is comparable. Similar to the previous cases, these violations can be removed by refining the lattice cell size and the time-step according to the stability criteria.

4.2 Two-dimensional problem with isotropic diffusion

Consider the domain $\Omega=(0,2)\times(0,1)$. We will take the diffusion coefficient as $D=5\times10^{-3}$ and the advection velocity to be $v_x = 1$ and $v_y = 0$. The initial concentration is zero. The boundary conditions are as follows:

$$u^p(x,y,t) = \begin{cases} 1, & x=0,\ \forall y,\ \forall t, \\ 0, & x=2,\ \forall y,\ \forall t, \end{cases} \tag{4.7a}$$

$$q^p(x,y,t) = 0, \quad y\in\{0,1\},\ \forall x,\ \forall t. \tag{4.7b}$$

The source term is set to be zero throughout the domain. We shall employ SRT LBM with a $D2Q4$ lattice model for numerical solution. The local method for enforcing the

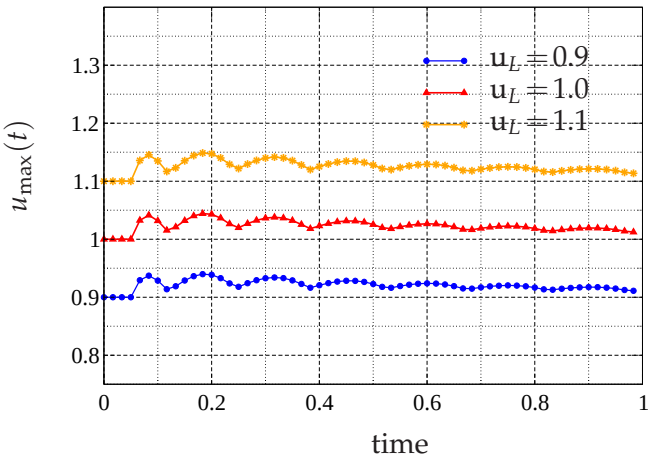
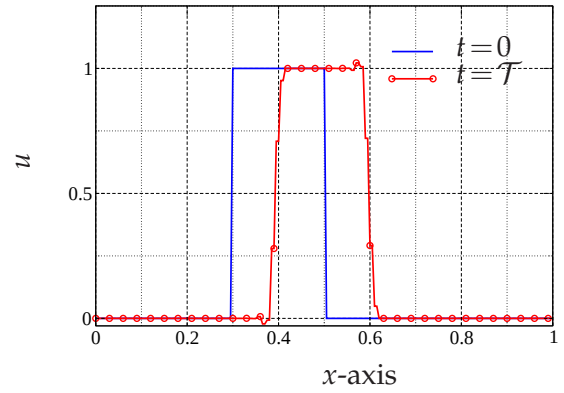
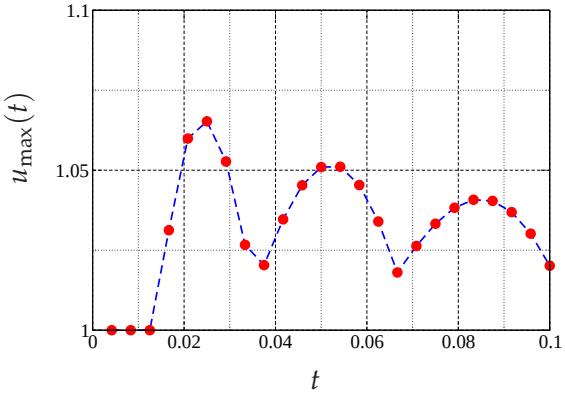


Figure 4: On comparison principle: This figure shows the maximum concentration observed against time. In all the cases, the maximum principle is violated. However, the comparison principle is satisfied.

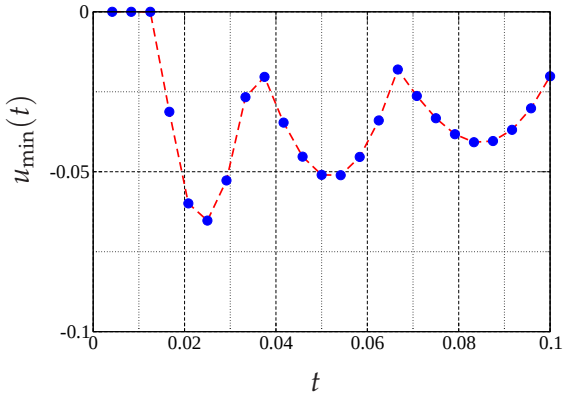
https://doi.org/10.4208/cicp.181015.270416a Published online by Cambridge University Press



(a) Concentration



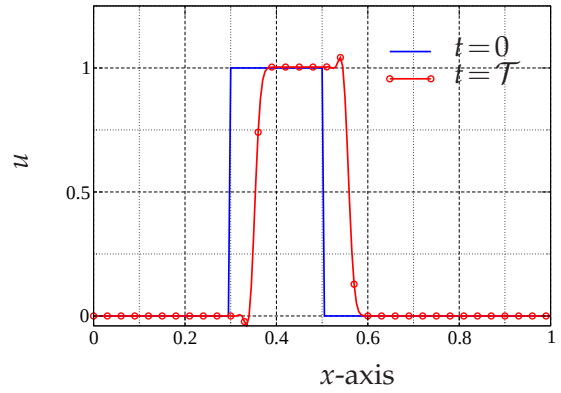
(b) Maximum observed concentration



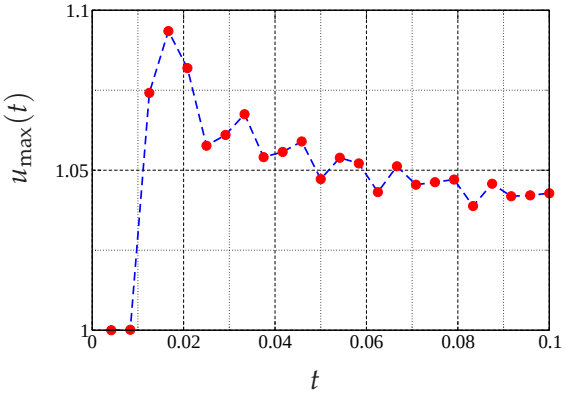
(c) Minimum observed concentration

Figure 5: On choice of lattice model: In this figure, the numerical results using the $D1Q2$ lattice are presented. This figure shows that the maximum principle is violated.

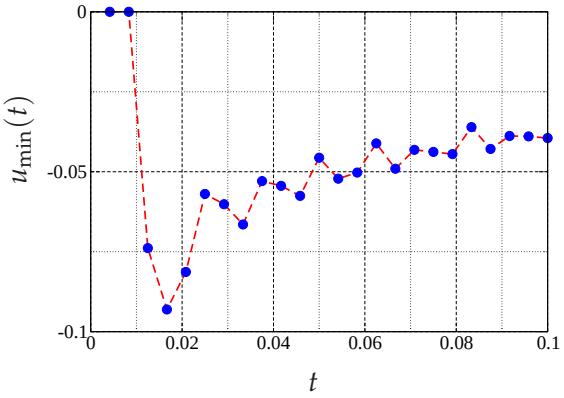
https://doi.org/10.4208/cicp.181015.270416a Published online by Cambridge University Press



(a) Concentration



(b) Maximum observed concentration



(c) Minimum observed concentration

Figure 6: On choice of lattice model: In this figure, the numerical results using the $D1Q3$ lattice are presented. The maximum principle is violated.

https://doi.org/10.4208/cicp.181015.270416a Published online by Cambridge University Press

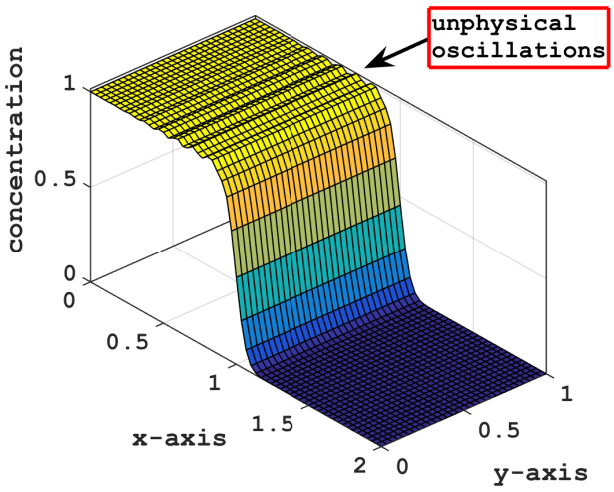


Figure 7: Two-dimensional problem with isotropic diffusion: This figure shows the unphysical node-to-node oscillations in the concentration. The maximum observed concentration in this figure is $u_{\max}(t=1)=1.0139$. The lattice cell size is $\Delta x=3.33\times10^{-2}$ and time-step is $\Delta t=1.85\times10^{-2}$. In this case the maximum principle is violated. This violation can be removed by grid refinement.

Dirichlet boundary condition at x$=$0 will be used (see Eq. (3.7)). The Dirichlet conditions at x$=$2 are enforced by the weighted splitting method (see Eq. (3.6)). Also, bounce-back conditions are posed to enforce zero flux boundary conditions (see Eq. (3.9)). The initial distributions are assigned to be the same as equilibrium distributions using the given initial concentration.

Fig. 7 shows the concentration at $t=1$. In this case, the cell size is $\Delta x=3.33\times10^{-2}$ and time-step is taken to be $\Delta t=1.85\times10^{-2}$. The maximum concentration in this case is $u_{\max}(t=1)=1.0139$, which is greater than the maximum possible value for concentration in this problem (the maximum principle is violated). These violations, however, can be removed by refining the cell size and the time-step according to a conventional Courant-Friedrichs-Lewy (CFL) [16] condition.

If we change the Dirichlet boundary conditions as follows

$$\mathrm{u^p(x,y,t)}=\begin{cases}0, & \mathrm{x}=0,\ \forall \mathrm{y},\ \forall \mathrm{t},\\ 1, & \mathrm{x}=2,\ \forall \mathrm{y},\ \forall \mathrm{t},\end{cases} \tag{4.8}$$

the spurious oscillations in the concentration profile lead to negative values. This result is shown in Fig. 8. The values of Δx and Δt are the same as before. The minimum observed value for concentration is $u_{\min}(t=1)=-0.0382$. Similar to the previous case, these oscillations can be removed by refining the lattice cell size and time-step.

https://doi.org/10.4208/cicp.181015.270416a Published online by Cambridge University Press

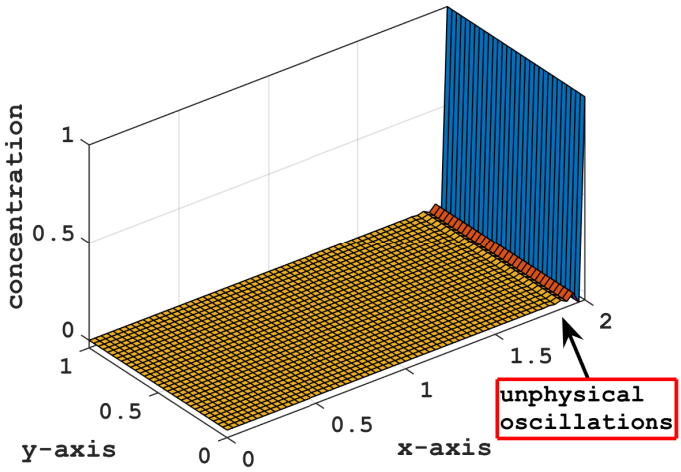


Figure 8: Two-dimensional problem with isotropic diffusion: This figure shows unphysical node-to-node oscillations in the concentration from the $D2Q4$ LBM. In this case, the numerical solution for the concentration adopts negative values. The minimum observed in this case is $u_{\min}(t=1)=-0.0384$.

4.3 Two-dimensional problem with anisotropic diffusion on a non-convex domain

We now examine the Y-N multiple-relaxation-time method for anisotropic diffusion tensor. The computational domain is shown in Fig. 9. We have taken $L=1$ and $\Gamma=\Gamma_{\text{outer}}\cup\Gamma_{\text{inner}}$. On the inner boundary, the concentration is prescribed to be unity (i.e., $u^{\text{p}}(\mathbf{x},t)=1 \text{ for } \mathbf{x}\in\Gamma_{\text{inner}}$). The flux is prescribed to be zero on the outer boundary (i.e., $q^{\text{p}}(\mathbf{x},t)=0 \text{ for } \mathbf{x}\in\Gamma_{\text{outer}}$). The anisotropic diffusion tensor is taken as:

$$\mathbf{D}(\mathbf{x})=\mathbf{R}_\theta^{\text{T}}\mathbf{D}_0\mathbf{R}_\theta, \tag{4.9}$$

where

$$\mathbf{D}_0=\begin{bmatrix} 10 & 0 \\ 0 & 10^{-3} \end{bmatrix}. \tag{4.10}$$

The orthogonal rotation matrix is denoted by $\mathbf{R}_\theta$, where θ denotes the angle of rotation. Herein, we have taken $\theta=\pi/4$. We employ the $D2Q5$ lattice model. The discrete velocity directions are given by

$$\boldsymbol{e}_i^{\text{T}}=\begin{cases} [0,0], & i=0, \\ c[\cos((i-1)\pi),\sin((i-1)\pi)], & i=1,2, \\ c[\cos((2i-5)\pi/2),\sin((2i-5)\pi/2)], & i=3,4, \end{cases} \tag{4.11}$$

where $c=\Delta x/\Delta t$. The respective weights are taken as:

$$w_i=\begin{cases} 1/3, & i=0, \\ 1/6, & i=1,2,3,4. \end{cases} \tag{4.12}$$

https://doi.org/10.4208/cicp.181015.270416a Published online by Cambridge University Press

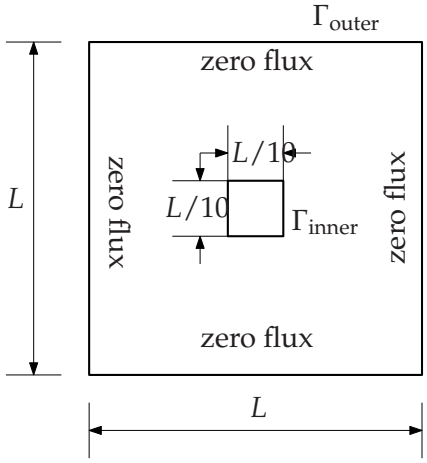


Figure 9: Two-dimensional problem with anisotropic diffusion in a non-convex domain: This figure provides a pictorial description of the test problem. A concentration of $u^p = 1$ is prescribed on the inner boundary Γ_{inner}.

The time interval of interest is taken as $\mathcal{T} = 10^{-2}$. We employ the local method of enforcing Dirichlet boundary conditions (see Eq. (3.7)). Table 2 provides the discretization parameters employed in this paper. Figs. 10-11 show that the Y-N method violates the non-negative constraint. In fact, the obtained minimum concentration is about -0.4, which is a significant violation given the fact that the concentration should be between 0 and 1. Another noticeable feature in all the cases considered, the minimum concentration converged to a negative value as the time progressed.

Table 2: Two-dimensional problem with anisotropic diffusion tensor on a non-convex domain: This table provides the minimum concentrations for various discretization parameters (i.e., Δx and Δt). We have taken $\Delta x^2 = \Delta t$.

Case	Δx	Δt	$u_{\min}(\mathcal{T})$
1	1.25×10^{-2}	1.5625×10^{-4}	-0.3781
2	1.00×10^{-2}	1.0000×10^{-4}	-0.4072
3	5.00×10^{-3}	2.5000×10^{-5}	-0.4044

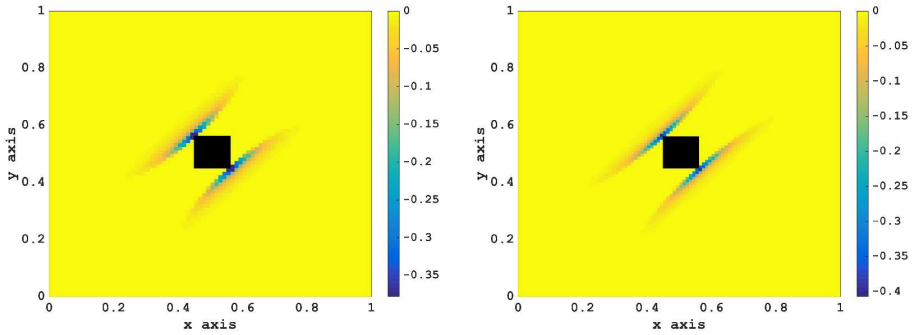
4.4 Two-dimensional problem with anisotropic and heterogeneous diffusion tensor

Consider the spatial domain to be $\Omega = (0,1)\times(0,1)$. We have taken the following anisotropic and heterogeneous diffusivity tensor:

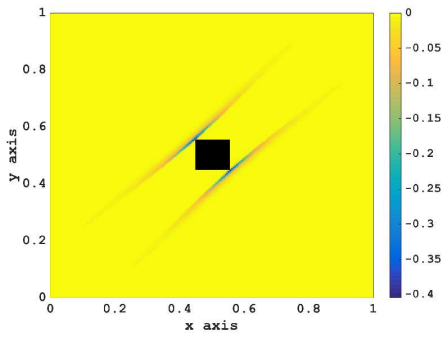
$$\mathbf{D}(x,y) = \epsilon' \mathbf{I}_2 + \begin{bmatrix} \epsilon x^2 + y^2 & -(1-\epsilon)xy \\ -(1-\epsilon)xy & x^2 + \epsilon y^2 \end{bmatrix}, \tag{4.13}$$

where $\epsilon \ll 1$ and $\epsilon' \ll 1$ are arbitrary constants, and $\mathbf{I}_2$ denotes the 2×2 identity matrix. For this numerical experiment, we have taken $\epsilon = 10^{-3}$ and $\epsilon' = 10^{-10}$. The prescribed

https://doi.org/10.4208/cicp.181015.270416a Published online by Cambridge University Press



(a) Case 1 (b) Case 2



(c) Case 3

Figure 10: Two-dimensional problem with anisotropic diffusion in a non-convex domain: The figure shows the regions where the non-negative constraint is violated under the Y-N method at $t = 0.01$. The concentration should be between 0 and 1.

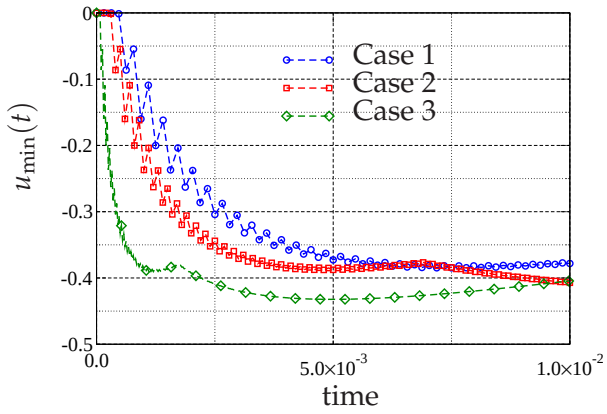


Figure 11: Two-dimensional problem with anisotropic diffusion in a non-convex domain: The figure shows the variation of minimum value of the concentration with respect to time under the Y-N multiple-relaxation-time lattice Boltzmann method. *It is evident from this numerical experiment that refining the discretization parameters, Δt and Δx, does not alleviate the violation of the non-negative constraint in the case of anisotropic diffusion.*

https://doi.org/10.4208/cicp.181015.270416a Published online by Cambridge University Press

concentration on the entire boundary is taken to be zero. The initial concentration is taken as:

$$\mathrm{u}_0(\mathrm{x},\mathrm{y}) = \begin{cases} 1, & (\mathrm{x},\mathrm{y}) \in [0.4,0.6] \times [0.4,0.6], \\ 0, & \text{otherwise.} \end{cases} \tag{4.14}$$

The time interval of interest is taken as $\mathcal{T} = 2.5 \times 10^{-2}$. The H-W method based on the $D2Q9$ lattice model is employed. The discrete velocities are taken as:

$$\boldsymbol{e}_i^{\mathrm{T}} = \begin{cases} [0,0], & i = 0, \\ c[\cos((i-1)\pi/2), \sin((i-1)\pi/2)], & i = 1,\cdots,4, \\ \sqrt{2}c[\cos((2i-9)\pi/4), \sin((2i-9)\pi/4)], & i = 5,\cdots,8, \end{cases}$$

with the following weights:

$$w_i = \begin{cases} 4/9, & i = 0, \\ 1/9, & i = 1,2,3,4, \\ 1/36, & i = 5,6,7,8. \end{cases} \tag{4.15}$$

The problem is solved using different choices of Δx and Δt, which are provided in Table 3. This table also provides insight on the performance of the H-W method. The following conclusions can be drawn from Figs. 13-14 and Table 3:

(a) The H-W multiple-relaxation-time method violates the non-negative constraint when the diffusion is anisotropic. Also, refining the discretization parameters does not alleviate violations of non-negative constraint. In fact, refinement may not lead to minimum concentrations closer to zero.

(b) As discussed earlier, the integral $\mathcal{J}_2$ should decrease monotonically with time for pure diffusion equations. But, the H-W method does not respect the decay property. However, it has been observed that refining the discretization parameters (i.e., Δx and Δt) can improve the performance of numerical solutions with respect to the decay property.

Table 3: Two-dimensional problem with anisotropic and heterogeneous diffusion tensor: In this table the values of discretization parameters for different cases is given. The nonnegative constraint is violated in all cases. Refining discretization parameters (Δt and Δx) does not remove the violations of the non-negative constraint.

Case	Δx	Δt	$u_{\min}(\mathcal{T})$	$u_{\max}(\mathcal{T})$
1	5.00×10^{-2}	1.00×10^{-3}	-0.0133	0.5167
2	2.50×10^{-2}	2.50×10^{-4}	-0.0077	0.5616
3	1.00×10^{-2}	4.00×10^{-5}	-0.0020	0.5977
4	5.00×10^{-3}	1.00×10^{-5}	-0.0001	0.5903

https://doi.org/10.4208/cicp.181015.270416a Published online by Cambridge University Press

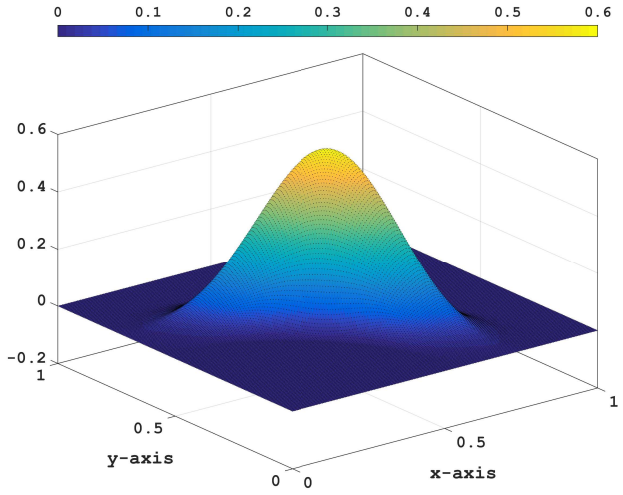
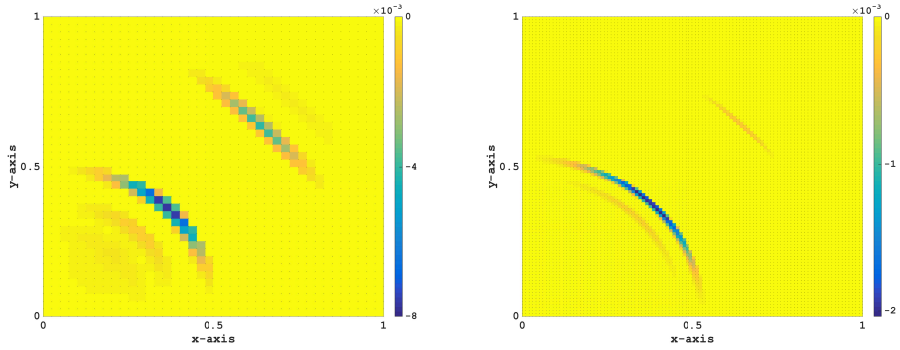


Figure 12: Two-dimensional problem with anisotropic and heterogeneous diffusion tensor: The concentration at time $t=0.025$ is shown. The values of discretization parameters are given in Table 3, Case 4. Even though by adjusting some parameters of the method, node-to-node oscillations can be alleviated the nodal concentration can adopt negative values. The minimum observed concentration in this case is $u_{\min}(\mathcal{T})=-0.0001$.



(a) Case 2 (b) Case 3

Figure 13: Two-dimensional problem with anisotropic and heterogeneous diffusion tensor: This figure shows the regions that have negative values for the concentration under the H-W method at $t=0.025$.

4.5 Fast bimolecular reaction in an anisotropic and heterogeneous medium

Consider a simple chemical reaction of the form:

$$n_A A + n_B B \rightarrow n_c C, \tag{4.16}$$

where A, B and C are the participating chemical species; and n_A, n_B and n_C are their respective stoichiometry coefficients. We are interested in the fate of the product C when

https://doi.org/10.4208/cicp.181015.270416a Published online by Cambridge University Press

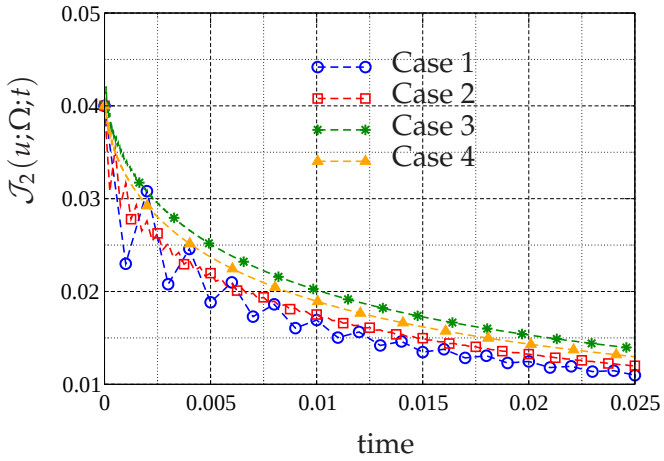


Figure 14: Two-dimensional problem with anisotropic and heterogeneous diffusion tensor: This figure shows the variation of the integral defined in Eq. (2.9) with respect to time under the H-W method. The simulation parameters are provided in Table 3. *It is evident from the figure that the H-W method violated the decay property.*

the time-scale of the chemical reaction is much faster than that of the transport processes (i.e., diffusion and advection). A detailed description of this mathematical model can be found in [31] and will not be repeated here. However, the mentioned paper neglected advection in all their numerical examples and the entire paper is devoted to the finite element method.

We will consider the domain given in Fig. 15. Dimensions of the domain are $L_{\mathrm{x}}=2$ and $L_{\mathrm{y}}=1$. The advection velocity is derived from the following stream function:

$$\psi(\mathrm{x},\mathrm{y})=-\mathrm{y}-\sum_{k=1}^{3}\alpha_k\cos\left(\frac{p_k\pi\mathrm{x}}{L_{\mathrm{x}}}-\frac{\pi}{2}\right)\sin\left(\frac{q_k\pi\mathrm{y}}{L_{\mathrm{y}}}\right),$$

where $(p_1,p_2,p_3)=(4,5,10)$, $(q_1,q_2,q_3)=(1,5,10)$, and $(\alpha_1,\alpha_2,\alpha_3)=(0.08,0.02,0.01)$. The dispersion tensor is taken as:

$$\mathbf{D}(\mathrm{x},\mathrm{y})=10^{-5}\mathbf{I}+\beta_{\mathrm{T}}\|\mathbf{v}\|\mathbf{I}+(\beta_{\mathrm{L}}-\beta_{\mathrm{T}})\frac{\mathbf{v}\otimes\mathbf{v}}{\|\mathbf{v}\|}, \tag{4.17}$$

where $\otimes$ denotes the tensor product, $\mathbf{I}$ is the 2×2 identity tensor, $\|\cdot\|$ is the 2-norm, $\beta_{\mathrm{T}}=10^{-4}$ and $\beta_{\mathrm{L}}=1$. The prescribed concentrations are $\mathrm{u}_A^{\mathrm{p}}=\mathrm{u}_B^{\mathrm{p}}=1$, and the stoichiometry coefficients are $n_A=1$, $n_B=2$ and $n_C=1$. The time interval of interest is $\mathcal{T}=2.5\times10^{-1}$. We employ the *D*2*Q*9 lattice model using the H-W method, and obtain the numerical solution for the fate of the product *C*. Discretization parameters for various cases are given in Table 4. *Figs.* 16-18 *clearly show that the H-W method violates the non-negative constraint, and the violations do not vanish either with time or with refinement of the discretization parameters.*

https://doi.org/10.4208/cicp.181015.270416a Published online by Cambridge University Press

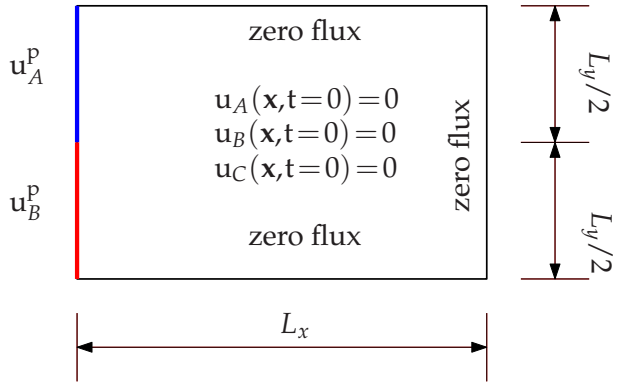


Figure 15: Fast bimolecular reaction in anisotropic and heterogeneous medium: This figure provides a pictorial description of the test problem. The reactants A and B undergo transport (i.e., both advection and diffusion) and reacts to give product C, which in turn gets transported. We take $L_x=2$ and $L_y=1$ in the numerical experiment.

Table 4: Fast bimolecular reaction in anisotropic and heterogeneous medium: Different discretization parameters and violation of the non-negative constraint.

Case	Δx	Δt	$u_{\min}(\mathcal{T})$	$u_{\max}(\mathcal{T})$
1	5.00×10^{-2}	2.50×10^{-4}	-0.0408	0.2612
2	2.50×10^{-2}	6.25×10^{-5}	-0.0455	0.3174
3	1.25×10^{-2}	1.56×10^{-6}	-0.0593	0.3217

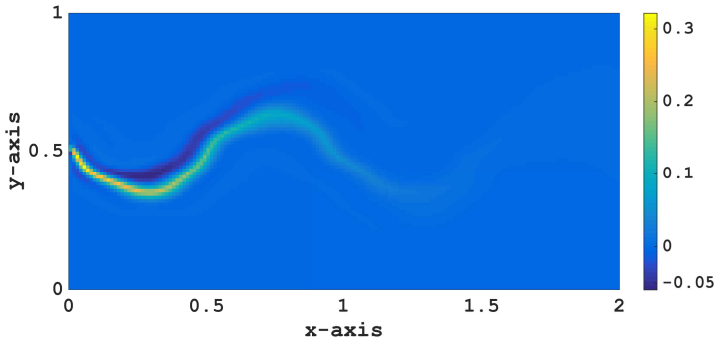
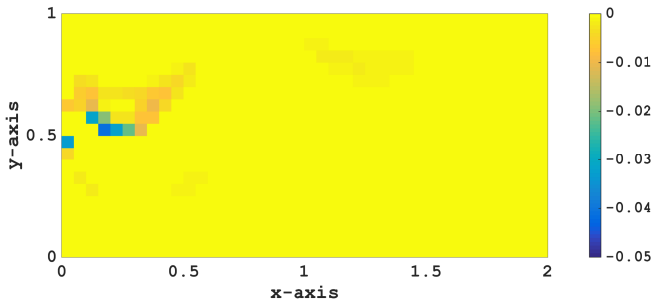


Figure 16: Fast bimolecular reaction in anisotropic and heterogeneous medium: The concentration of the chemical species C at time $t=0.1$ is shown. Violation of the non-negative constraint is obvious.

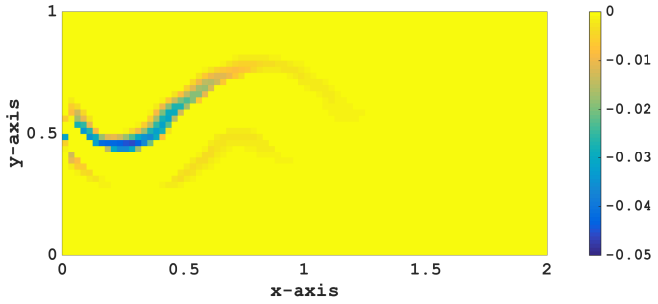
5 A simple theoretical analysis

In this section, we will provide a simple criterion in terms of the discretization parameters to satisfy the non-negative constraint for one-dimensional problems. We will also limit our scope to pure diffusion equations (i.e., $\mathbf{v}(\mathbf{x},t)=\mathbf{0}$), and $\partial\Omega=\Gamma^D$. We will restrict the

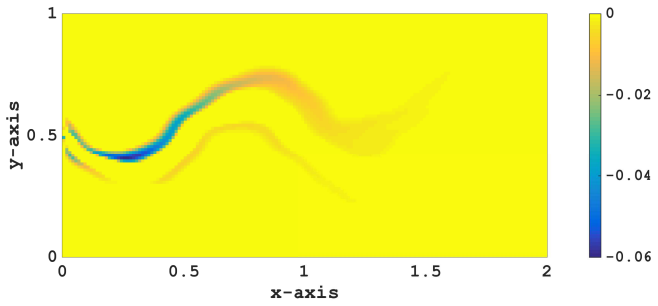
https://doi.org/10.4208/cicp.181015.270416a Published online by Cambridge University Press



(a) Case 1



(b) Case 2



(c) Case 3

Figure 17: Fast bimolecular reaction in anisotropic and heterogeneous medium: This figure shows the regions where the concentration of the product C is negative at $t=\mathcal{T}=0.1$ under the H-W method. The parameters for various cases are provided in Table 4. The violations appear at large number of lattice nodes, and are spread across the computational domain.

analysis to the $D1Q3$ lattice model. We initialize the discrete distributions f_i at all lattice nodes as follows:

$$f_i(x,t=0)=w_i\mathrm{u}_0(x). \tag{5.1}$$

Since $w_i>0$ and $\mathrm{u}_0(x)\geq 0$, we have $f_i(x,0)\geq 0$. Furthermore, we assume that the Dirichlet boundary conditions will be discretized using the *weighted splitting method* (see Eq. (3.6)). The weighted splitting method guarantees the non-negativity of distributions f_i for a

https://doi.org/10.4208/cicp.181015.270416a Published online by Cambridge University Press

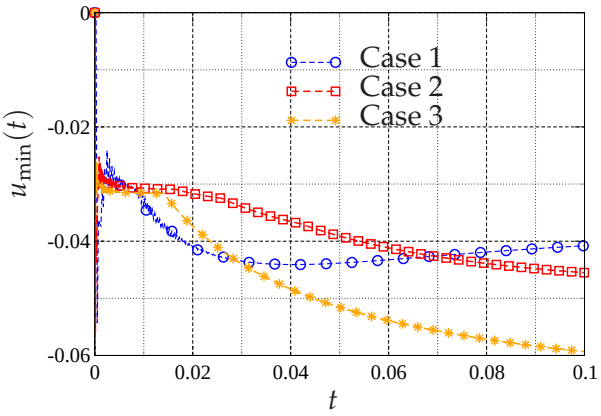


Figure 18: Fast bimolecular reaction in anisotropic and heterogeneous medium: The minimum concentration of the product C is plotted against time for various cases whose simulation parameters are provided in Table 4. *This figure clearly illustrates that refining the discretization parameters does not eliminate the violation of the non-negative constraint under the H-W method.*

lattice node on the boundary provided that the prescribed concentration on Γ^{D} is non-negative. That is,

$$\mathrm{u}^{\mathrm{p}}(x\in\Gamma^{\mathrm{D}},t)\geq 0 \;\Rightarrow\; f_i(x\in\Gamma^{\mathrm{D}},t)\geq 0. \tag{5.2}$$

So far, we have made sure that all the distributions at the previous time-level are non-negative, and the discretization of the boundary conditions will not disrupt the non-negativity of distributions. Since the distributions at time t are non-negative, equilibrium distributions f_i^{eq} will be non-negative in the calculation of the collision step at time $t+\Delta t$. That is,

$$\begin{aligned} f_i(x,t)\geq 0 &\Rightarrow u(\boldsymbol{x},t)=\sum_i f_i(x,t)\geq 0\\ &\Rightarrow f_i^{\mathrm{eq}}(\boldsymbol{x},t)=w_i u(\boldsymbol{x},t)\geq 0. \end{aligned} \tag{5.3}$$

If all of these conditions are satisfied, restricting the value of the relaxation time τ can lead to non-negative concentrations at all lattice nodes and for all time-levels. That is if the following conditions hold for terms in Eq. (3.2), then the value of f_i in the next time-level will be non-negative as well

$$|f_i\rangle(\boldsymbol{x}+\boldsymbol{e}_i\Delta t,t+\Delta t)=\underbrace{\left(1-\frac{1}{\tau}\right)}_{\geq 0}\underbrace{|f_i\rangle(\boldsymbol{x},t)}_{\geq 0}+\frac{1}{\tau}\underbrace{|f_i^{\mathrm{eq}}\rangle(\boldsymbol{x},t)}_{\geq 0}, \tag{5.4}$$

hence, we require that

$$1-1/\tau\geq 0. \tag{5.5}$$

https://doi.org/10.4208/cicp.181015.270416a Published online by Cambridge University Press

Using Eq. (3.3) and the above inequality, one can obtain the following condition that ensures non-negativity:

$$\Delta t \geq \frac{\Delta x^2}{6\mathrm{D}}. \tag{5.6}$$

That is, if the discretization parameters, Δt and Δx, satisfy inequality (5.6) then all the distributions f_i will be non-negative. Non-negativity of all f_i's implies the non-negativity of the concentration $u(\boldsymbol{x},t)$, which stems directly from Eq. (3.5).

Note that this result is only valid for one-dimensional pure diffusion equation (i.e., the advection velocity is zero) and for $D1Q3$ lattice model. However, for the typical lattice models and isotropic diffusion tensor and $\|\mathbf{v}(\mathbf{x},t)\| \ll c_s$, a similar result can be drawn. The inequality in Eq. (5.5) implies that

$$\Delta t \leq \frac{2\mathrm{D}}{c_s^2}. \tag{5.7}$$

Assuming that the boundary conditions do not introduce any negative distributions, then this condition on discretization parameters ensures non-negativity of concentration. Note that c_s depends on the lattice model. It needs to be emphasized that the above conditions do not guarantee the preservation of the comparison principles. Deriving similar conditions for more sophisticated lattice models in two and three dimensions and for multiple-relaxation-time methods will require a more rigorous analysis.

Another noteworthy point is that we have put stronger conditions on the values of distributions f_i in order to meet the non-negative constraint for the concentration. In other words, for nodal concentrations to be non-negative we made sure that all the distributions are non-negative (i.e., $f_i(\boldsymbol{x},t) \geq 0 \,\forall i$). However, this condition can be relaxed by allowing some of the f_i to be negative, but with an additional constraint that $\sum_{i=0}^{m-1} f_i(\boldsymbol{x},t) \geq 0$. We do not pursue such an approach here, but one can consider them in future developments of lattice Boltzmann methods.

A careful look into the literature does provide instances of the violation of the non-negative constraint under the LBM. For example, see [24, Figure 9] and [37, Figures 8–10]. Even though the methods presented in these references are stable and converge to the advection-diffusion equation, they do not preserve the maximum principle. One of the earlier approaches to avoid negative values for discrete populations in the lattice Boltzmann method is presented in [26]. However, it has been shown that this method may not conserve monotonicity in entropy production [44]. A recent work that provides thorough mathematical analysis based on L^∞ convergence of the LBM solution and preservation of maximum principle for one-dimensional diffusion equation is presented in [17]. As of now, there are no clear-cut guidelines to extend the approach proposed in [17] to anisotropic diffusion. Another notable approach is to equip the lattice Boltzmann method with the Boltzmann's H function in order to guarantee the non-negativity of the discrete distributions [6, 13, 25]. Recently, multi-block LBMs have proven to be successful in removing spurious oscillations (e.g., from the solution for pressure field) in the LBM solution for the viscous flow problems [28, 47, 48]. Hence, an interesting effort would be

https://doi.org/10.4208/cicp.181015.270416a Published online by Cambridge University Press

to extend those techniques to isotropic and anisotropic advection-diffusion problems in order to control the spurious modes from the LBM solution. It should be noted that occurrence of negative distributions, is not unique to the solution of advection-diffusion equation, but may also happen in numerical solution of various flow problems. Negative values of discrete populations from LBM may result in negative values for mass density, which is clearly unphysical. This certainly demands a systematic analysis, which can be a subject matter for future research.

6 Concluding remarks

The maximum and comparison principles are two important mathematical properties of diffusion-type equations. The non-negative constraint is an important physical constraint on the concentration in transport and reactive-transport equations. There are other properties that the solutions to diffusion-type equations satisfy under appropriate conditions on the input data; for example, the decay property. A main challenge in designing a predictive numerical formulation is to satisfy these mathematical principles and physical constraints in the discrete setting. In this paper, using representative numerical examples, we have systematically documented that the current LBM-based formulations do not satisfy the maximum principle, the comparison principle, the non-negative constraint, and the decay property. We have also shown that the discretization of boundary conditions has an effect on the performance of the lattice Boltzmann method in meeting these properties. To this end, we proposed a way of discretizing Dirichlet boundary conditions – the weighted splitting method. We then derived a theoretical bound in terms of the time-step and lattice cell size that guarantees non-negative values for the concentration under the weighted splitting method for one-dimensional problems.

It needs to be emphasized that stability conditions for the lattice Boltzmann method (i.e., Courant-Friedrichs-Lewy conditions) have been satisfied in all our numerical experiments. *This implies that meeting stability conditions alone does not guarantee the preservation of the mentioned mathematical principles in the discrete setting.* The main findings of the paper about LBM-based formulations can be summarized as follows:

(a) One-dimensional problems: For a given time-step, one can eliminate the violation of the non-negative constraint and the maximum principle by refining the lattice cell size. For a given lattice cell size, the violation of the non-negative constraint and the maximum principle cannot be eliminated by decreasing the time-step. Both these trends are similar to FEM, which have been reported in [32].

(b) Critical time-step: Based on a simple theoretical analysis, we found that $\Delta t \geq \Delta x^2/(6D)$ in order to meet the non-negative constraint under LBM for 1D problems. One can obtain exactly the same bound under the single-field Galerkin finite element method based on the backward Euler time-stepping scheme for 1D problems [32]. This is an interesting result given the fact that the underlying basis of the lattice Boltzmann method (which solves Boltzmann equation to obtain distributions at lattice nodes)

https://doi.org/10.4208/cicp.181015.270416a Published online by Cambridge University Press

is completely different from that of the finite element method (which is based on a weak formulation).

(c) Isotropic vs. anisotropic diffusion: The violations of the non-negative constraint and the maximum principle are smaller in magnitude and smaller in terms of spatial extent when the diffusion is isotropic. Also, for a given time-step, one can decrease these violations by refining the lattice cell size in the case of isotropic diffusion. On the other hand, neither decreasing the time-step nor refining the lattice cell size will eliminate the violation of the non-negative constraint for anisotropic diffusion.

(d) Non-convex domains: The magnitudes of the violation of the non-negative constraint are larger for non-convex domains. However, it needs to be emphasized that one may have violations even on convex domains.

(e) Comparison principle: The comparison and maximum principles should be accounted for separately. Satisfaction of one does not lead to satisfaction of the other.

(f) Decay property: The LBM-based formulations, in general, violate the decay property.

(g) The lattice Boltzmann method does not posses a variational structure similar to the one possessed by the finite element method. Due to this reason, the non-negative formulations proposed under the finite element method (e.g., [32]) cannot be directly extended to the lattice Boltzmann method.

(h) The only procedure that is available to meet the non-negative constraint under the lattice Boltzmann method for anisotropic diffusion, is the clipping procedure, which basically chops off the negative values. But, this procedure fixes neither the violation of the decay property nor the violation of the comparison principle. Moreover, this method does not have any physical or mathematical basis, and it is rather *ad hoc*.

One may wonder how important properties such as the maximum principle or the non-negative constraint are violated. Several works have shown that the LBM "converges" to Eq. (2.3). The answer lies in the fact that there are different notions of convergence and all of them are not equivalent. Strong notions of convergence such as the uniform convergence may not be assessed using the current tools of analysis in the LBM literature. For a careful treatment of convergence see [3, 45]. In order to satisfy maximum principles and the non-negative constraint in the discrete setting, one needs to address uniform convergence, and the mean-square (or weak) convergence will not suffice [14, 15]. Most of the studies that performed convergence analysis of the LBM have employed the classical Chapman-Enskog procedure. However, it is imperative to recognize that the classical Chapman-Enskog procedure does not establish uniform convergence. In fact, a known drawback of the Chapman-Enskog procedure is that it can introduce spurious oscillations, which are not present in the exact solution. For example, a beautiful discussion on this issue can be found in [8].

A future research direction could be development of LBM-based formulations for diffusion and advection-diffusion equations that respect the maximum and comparison principles, and meet the non-negative constraint. This paper can also serve as a source of benchmark problems for such a research endeavor.

https://doi.org/10.4208/cicp.181015.270416a Published online by Cambridge University Press

Appendix

A MATLAB [1] code for the one-dimensional *advection and diffusion of the Gaussian hill* in Section IV is provided.

```
%---problem paramteres
q = 2;
xL = -2.0;
xR = 2.0;
L = xR - xL;
T = 0.5;  %time interval of interest
D = 0.01; %diffusion coefficient
v = -1.0; %advection velocity
qL = 0.0; %prescribed flux at x = xL
qR = 0.0; %prescribed flux at x = xR

%---LBM discretization
Nx = 160;
dx = L/Nx; %spatial discretization
dt = dx^2/(6*D);     %time-step
Nt = ceil(T/dt);  %number of time-steps
c_s = dx/dt;     %lattice velocity
omega = 1/(0.5 + D*dt/dx^2);     %relaxation
f = zeros(Nx,q);
e = [1, -1];   %discrete velocities
w = [0.5, 0.5];     %weights
u = zeros(Nx,1);
x = zeros(1,Nx);
uMin = zeros(1,Nt);
uMax = zeros(1,Nt); uMax(1) = 1;

%---initial values
for n = 1 : Nx
    x(n) = xL + (n-1)*dx;
    u(n) = 0.9*exp(-(x(n) - 0.75)^2/0.001);
    f(n,:) = w*u(n)*(eye(2) + ...
                     diag(e)*v/c_s);
end

%---time stepping
for t = 2 : Nt
   %---stream and collide
```

https://doi.org/10.4208/cicp.181015.270416a Published online by Cambridge University Press

```
    u = sum(f,2);
    feq = u*w*(eye(2) + diag(e)*v/c_s);
    f = (1 - omega)*f + omega*feq;
    f(:,1) = circshift(f(:,1),e(1));
    f(:,2) = circshift(f(:,2),e(2));
    %---boundary conditions/bounce-back
    f(1,1) = f(1,2); f(Nx,2) = f(Nx,1);
    %---storing min and max observed values
    uMin(t) = min(u);
    uMax(t) = max(u);
end

figure
subplot(2,1,1)
plot((1:Nt)*dt, uMin);
subplot(2,1,2)
plot((1:Nt)*dt, uMax);
```

Acknowledgments

The authors acknowledge the support from the National Science Foundation through the Grant No. CMMI 1068181. The opinions expressed in this paper are those of the authors and do not necessarily reflect that of the sponsor(s).

References

[1] *MATLAB R2014b*. The MathWorks, Inc., Natick, Massachusetts, 2014.
[2] S. G. Ayodele, F. Varnik, and D. Raabe. Lattice Boltzmann study of pattern formation in reaction-diffusion systems. *Physical Review E*, 83:016702, 2011.
[3] G. Bachman and L. Narici. *Functional Analysis*. Dover Publications, New York, second edition, 1998.
[4] J. Bear, C. Tsang, and G. De Marsily. *Flow and Contaminant Transport in Fractured Rock*. Academic Press, San Diego, 2012.
[5] P. L. Bhatnagar, E. P. Gross, and M. Krook. A model for collision processes in gases. I. Small amplitude processes in charged and neutral one-component systems. *Physical Review*, 94(3):511, 1954.
[6] B. M. Boghosian, J. Yepez, P. V. Coveney, and A. Wager. Entropic lattice Boltzmann methods. In *Proceedings of the Royal Society of London A: Mathematical, Physical and Engineering Sciences*, 457:717–766, 2001.
[7] M. L. Brusseau. Transport of reactive contaminants in heterogeneous porous media. *Reviews of Geophysics*, 32(3):285–313, 1994.
[8] C. Cercignani. *The Boltzmann Equation and its Applications*. Springer, New York, 1988.

https://doi.org/10.4208/cicp.181015.270416a Published online by Cambridge University Press

[9] Z. Chai and T. S. Zhao. Lattice Boltzmann model for convection-diffusion equation. *Physical Review E*, 87:63309, 2013.
[10] S. Chapman and T. G. Cowling. *The Mathematical Theory of Non-uniform Gases: An Account of the Kinetic Theory of Viscosity, Thermal Conduction and Diffusion in Gases*. Cambridge University Press, Cambridge, 1970.
[11] Q. Chen, X. Zhang, and J. Zhang. Improved treatments for general boundary conditions in the lattice Boltzmann method for convection-diffusion and heat transfer processes. *Physical Review E*, 88 (3):033304, 2013.
[12] S. Chen and G. D. Doolen. Lattice Boltzmann methods for fluid flows. *Annual Review of Fluid Mechanics*, 30:329–364, 1998.
[13] S. S. Chikatamarla and I. V. Karlin. Entropic lattice Boltzmann method for multiphase flows. *Physical Review Letters*, 114(17):174502, 2015.
[14] P. G. Ciarlet. Discrete maximum principle for finite-difference operators. *Aequationes Mathematicae*, 4:338–352, 1970.
[15] P. G. Ciarlet and P-A. Raviart. Maximum principle and uniform convergence for the finite element method. *Computer Methods in Applied Methods and Engineering*, 2:17–31, 1973.
[16] R. Courant, K. Friedrichs, and H. Lewy. Über die partiellen Differenzengleichungen der mathematischen Physik. *Mathematische Annalen*, 100(1):32–74, 1928.
[17] S. Dellacherie. Construction and analysis of lattice Boltzmann methods applied to a 1D convection-diffusion equation. *Acta Applicandae Mathematicae*, 131(1): 69–140, 2014.
[18] D. d'Humières. Multiple–relaxation–time lattice Boltzmann models in three dimensions. *Philosophical Transactions of the Royal Society of London A: Mathematical, Physical and Engineering Sciences*, 360(1792):437–451, 2002.
[19] L. C. Evans. *Partial Differential Equations*. American Mathematical Society, Providence, Rhode Island, 1998.
[20] G. Falcucci, S. Ubertini, C. Biscarini, S. Di Francesco, D. Chiappini, S. Palpacelli, A. De Maio, and S. Succi. Lattice Boltzmann methods for multiphase flow simulations across scales. *Communications in Computational Physics*, 1:1–35, 2006.
[21] S. Harris. *An Introduction to the Theory of the Boltzmann Equation*. Dover Publications, Mineola, 2004.
[22] X. He and L. Lou. Theory of the lattice Boltzmann method: From the Boltzmann equation to the lattice Boltzmann equation. *Physical Review E*, 56:6811, 1997.
[23] R. Huang and H. Wu. A modified multiple-relaxation-time lattice Boltzmann model for convection-diffusion equation. *Journal of Computational Physics*, 274:50–63, 2014.
[24] R. Huang and H. Wu. Lattice Boltzmann model for the correct convection-diffusion equation with divergence-free velocity field. *Physical Review E*, 91(3):033302, 2015.
[25] I. V. Karlin, S. Ansumali, C. E. Frouzakis, and S. S. Chikatamarla. Elements of the lattice Boltzmann method I: Linear advection equation. *Communications in Computational Physics*, 1(4):616–655, 2006.
[26] Y. Li, R. Shock, R. Zhang, and H. Chen. Numerical study of flow past an impulsively started cylinder by the lattice-Boltzmann method. *Journal of Fluid Mechanics*, 519:273–300, 2004.
[27] R. Liska and M. Shashkov. Enforcing the discrete maximum principle for linear finite element solutions for elliptic problems. *Communications in Computational Physics*, 3:852–877, 2008.
[28] H. Liu, J. G. Zhou, and R. Burrows. Multi-block lattice Boltzmann simulations of subcritical flow in open channel junctions. *Computers & Fluids*, 38(6):1108–1117, 2009.
[29] K. Malek and M. Coppens. Knudsen self- and Fickian diffusion in rough nanoporous media.

https://doi.org/10.4208/cicp.181015.270416a Published online by Cambridge University Press

The Journal of Chemical Physics, 119(5):2801–2811, 2003.
[30] K. B. Nakshatrala and A. J. Valocchi. Non-negative mixed finite element formulations for a tensorial diffusion equation. *Journal of Computational Physics*, 228:6726–6752, 2009.
[31] K. B. Nakshatrala, M. K. Mudunuru, and A. J. Valocchi. A numerical framework for diffusion-controlled bimolecular-reactive systems to enforce maximum principles and the non-negative constraint. *Journal of Computational Physics*, 253:278–307, 2013a.
[32] K. B. Nakshatrala, H. Nagarajan, and M. Shabouei. A numerical methodology for enforcing maximum principles and the non-negative constraint for transient diffusion equations. *Communications in Computational Physics*, 19:53–93, 2016.
[33] C. V. Pao. *Nonlinear Parabolic and Elliptic Equations*. Springer-Verlag, New York, 1993.
[34] M. H. Protter and H. F. Weinberger. *Maximum Principles in Differential Equations*. Springer-Verlag, New York, 1999.
[35] A. F. Di Rienzo, P. Asinari, E. Chiavazzo, N. I. Prasianakis, and J. Mantzaras. Lattice Boltzmann model for reacting flow simulations. *Europhysics Letters*, 98:34001, 2012.
[36] W. M. Saltzman. *Drug Delivery: Engineering Principles for Drug Therapy*. Oxford University Press, New York, 2001.
[37] B. Servan-Camas and F. T. C. Tsai. Non-negativity and stability analyses of lattice Boltzmann method for advection–diffusion equation. *Journal of Computational Physics*, 228(1):236–256, 2009.
[38] B. Shi and Z. Guo. Lattice Boltzmann model for nonlinear convection-diffusion equations. *Physical Review E*, 79:16701, 2009.
[39] J. Siepmann and F. Siepmann. Mathematical modeling of drug delivery. *International Journal of Pharmaceutics*, 364(2):328–343, 2008.
[40] P. A. Skordos. Initial and boundary conditions for the lattice Boltzmann method. *Physical Review E*, 48(6):4823, 1993.
[41] C. I. Steefel, D. J. DePaolo, and P. C. Lichtner. Reactive transport modeling: An essential tool and a new research approach for the Earth sciences. *Earth and Planetary Science Letters*, 240:539 – 558, 2005.
[42] M. Stiebler, J. Tolke, and M. Krafczyk. Advection-diffusion lattice Boltzmann scheme for hierarchical grids. *Computers and Mathematics with Applications*, 55:1576–1584, 2008.
[43] S. Succi. *The Lattice Boltzmann Equation for Fluid Dynamics and Beyond*. Oxford University Press, Oxford, 2001.
[44] F. Tosi, S. Ubertini, S. Succi, H. Chen, and I. V. Karlin. Numerical stability of entropic versus positivity-enforcing lattice Boltzmann schemes. *Mathematics and Computers in Simulation*, 72(2):227–231, 2006.
[45] M. T. Vaughn. *Introduction to Mathematical Physics*. Wiley-VCH, Weinheim, 2007.
[46] H. Yoshida and M. Nagaoka. Multiple-relaxation-time lattice Boltzmann model for the convection and anisotropic diffusion equation. *Journal of Computational Physics*, 229:7774–7795, 2010.
[47] D. Yu and S. S. Girimaji. Multi-block lattice Boltzmann method: Extension to 3D and validation in turbulence. *Physica A: Statistical Mechanics and its Applications*, 362(1):118–124, 2006.
[48] D. Yu, R. Mei, and W. Shyy. A multi-block lattice Boltzmann method for viscous fluid flows. *International Journal for Numerical Methods in Fluids*, 39(2):99–120, 2002.
[49] Q. Zou and X. He. On pressure and velocity boundary conditions for the lattice Boltzmann BGK model. *Physics of Fluids*, 9(6):1591–1598, 1997.

https://doi.org/10.4208/cicp.181015.270416a Published online by Cambridge University Press